NIH Public Access
Author Manuscript
Neuroreport. Author manuscript; available in PMC 2013 July 23.

Published in final edited form as:
Neuroreport. 2011 August 24; 22(12): 623–627. doi:10.1097/WNR.0b013e3283497334.

Retinal amyloid peptides and complement factor H in transgenic models of Alzheimer's disease

Peter N. Alexandrov[a], **Aileen Pogue**[b], **Surjyadipta Bhattacharjee**[b], and **Walter J. Lukiw**[b]

[a]Russian Academy of Medical Sciences, Moscow, Russia

[b]LSU Neuroscience Center and Department of Ophthalmology, Louisiana State University Health Sciences Center, New Orleans, Louisiana, USA

Abstract

Murine transgenic models of Alzheimer's disease (Tg-AD) have been useful to analyze the contribution of β-amyloid precursor protein (βAPP), Aβ42 peptide deposition, and the proinflammatory mechanisms that characterize Alzheimer-type neuropathology. In this report, we have studied the levels of βAPP, Aβ40 and Aβ42 peptide, as well as the innate immune and inflammatory response-regulator complement factor H in the brain and retina in four different Tg-AD models including Tg2576, PSAPP, 3xTg-AD, and 5xFAD. Aged, symptomatic 5xFAD mice showed the highest retinal abundance of Aβ42 peptides and the highest deficits in complement factor H. This may be a useful model to study the mechanisms of amyloidmediated inflammatory degeneration. The superior colliculus and retina obtained from late-stage Alzheimer's disease revealed upregulated amyloidogenic and inflammatory signaling along the anteroposterior axis of the retinal-primary visual cortex pathway.

Keywords

5xFAD; age-related macular degeneration; Alzheimer's disease; inflammatory neurodegeneration; miRNA-146a; retina; Tg2576; transgenic models of Alzheimer's disease

Introduction

Alterations in beta-amyloid precursor protein (βAPP) processing into amyloid-beta (Aβ) peptides, and deficits in the expression of the innate immune-repressor complement factor H (CFH), underlie the amyloidogenic and inflammatory neuropathology characteristic of age-related degeneration of the retina and Alzheimer's disease of the brain [1–7]. Substantial evidence further supports impairments in visual function in patients with Alzheimer's disease extending from targeted ganglion cell atrophy and loss in the retina to increased inflammatory neurodegeneration in the primary visual cortex (PVC; Brodmann area A17) [8,9]. Visual spatial impairment and thinning of the retinal ganglion fiber layer may be one of the earliest symptoms of Alzheimer's disease-type neurodegenerative change [10,11]. Disturbances in visual signal processing, including hallucinations and related perceptive disturbances within the visual field, is a commonly reported feature of an end-stage Alzheimer's disease [8–11]. A number of transgenic murine models of Alzheimer's disease (Tg-AD) are currently available to investigate amyloidogenic and inflammatory mechanisms

© 2011 Wolters Kluwer Health | Lippincott Williams & Wilkins.

Correspondence to Walter J. Lukiw, MS, PhD, LSU Neuroscience Center of Excellence, Louisiana State University Health Sciences Center, 2020 Gravier Street, Suite 904, New Orleans, LA 70112-2272, USA, Tel: +1 504 599 0842; fax: + 1 504 568 5801; wlukiw@lsuhsc.edu.

NIH-PA Author Manuscript
NIH-PA Author Manuscript
NIH-PA Author Manuscript

NIH-PA Author Manuscript

NIH-PA Author Manuscript

NIH-PA Author Manuscript

in the development of Alzheimer's disease, including the Tg2576, PSAPP, 3xTg-AD, and 5xFAD models that overexpress amyloid and acquire Alzheimer-type neuropathology as they age (Fig. 1) [2,14–20]. As Aβ42-peptide accumulation in Tg-AD retina may contribute to retinal degeneration and Alzheimer visual impairment, in this study, we investigated differences in the cerebrovascular-associated Aβ40 peptide, the strongly aggregating amyloidogenic Aβ42 peptide, and the CFH in four Tg-AD models in brain and retinal tissues. Interestingly, brain and retinal tissues obtained from late-stage, short post-mortem interval Alzheimer samples showed significantly upregulated inflammatory signaling along three major nodes of the retinal PVC circuit. These data indicate that in symptomatic Tg-AD animals and in Alzheimer's disease, markers for both amyloidosis and inflammation are apparent, extending along the anteroposterior axis from the retina, and suggest the global involvement of Alzheimer-like neuropathology and retinopathology along the retinal–cortical axis.

Materials and methods

Reagents, brain, and retinal tissues

Reagents used in these experiments were obtained from commercial suppliers and were used without further purification [3,5–8,14]. Samples of age-matched control and Alzheimer brain and retinal tissues, and the retina and cortex of control and symptomatic (i.e., exhibiting Alzheimer-type neuropathology) Tg-AD animals, Tg2576, PSAPP, 3xTg-AD, and 5xFAD, were analyzed for βAPP and CFH abundance using western analysis as previously described [3,5–8]. All Alzheimer's disease cases were late stage; the apolipoprotein E genotype of the Alzheimer samples were either E2/E4 or E3/E4 [3,5]. The mean (± one standard deviation) age of the human control brain group (N=6) was 71.5±6.1 years and the mean postmortem interval (death-to-brain freezing interval) was 3 h; the mean age of the Alzheimer brain group (N=6) was 72.2±7.6 years, and the mean postmortem interval was 3.1 h. Further details on the RNA quality control for these human brain samples have been recently published [5].

Total RNA and protein extraction and quality control

Total RNA and proteins were simultaneously isolated using TRIzol reagent (Invitrogen, Carlsbad, California, USA). As an index of tissue integrity, RNA quality was assessed using an Agilent Bioanalyzer 2100 (Lucent Technologies/Caliper Technologies, Palo Alto, California, USA); typically one microliter of total RNA sample was loaded on the RNA chip (6000 Nano Labchip; Caliper Technologies) and was analyzed for quality control [3,5,6]. Protein concentrations were determined using dotMETRIC microassay as previously described (sensitivity 0.3 ng protein/ml; Chemicon- Millipore, Billerica, Massachusetts, USA) [3,5,6].

Enzyme-linked immunosorbent assay and western analysis

Enzyme-linked immunosorbent assay (ELISA) was performed for quantification of Aβ40 and Aβ42 peptides in control and transgenic mouse brain and retina as previously described [13,21]. Western immunoblots were performed using murine-specific and/or human-specific primary antibodies directed against the control protein marker β-actin (3598–100; Sigma-Aldrich Chemical Company, St Louis, Missouri, USA), human βAPP (C-20; sc-7000), or CFH (H-7; sc-166613H-5; sc-166608; Santa Cruz Biotechnologies, Santa Cruz, California, USA) using methods previously described by our group [3,6,22,23].

NIH-PA Author Manuscript

NIH-PA Author Manuscript

NIH-PA Author Manuscript

Statistical analysis and data interpretation

All statistical procedures for protein (western) abundance were analyzed using a two-way factorial analysis of variance (*P*) using programs and procedures in the SAS language (Statistical Analysis Institute, Cary, North Carolina, USA) and as previously described [3,5,6,9]. Only *P* values of less than 0.05 (analysis of variance) were considered to be statistically significant. Figures were generated using Excel 2008 (Microsoft Corporation, Redmond, Washington, USA), Adobe Illustrator CS3 version 11.0, and Photoshop CS2 version 9.0.2 (Adobe, San Jose, California, USA).

Results

Aβ40 and Aβ42 peptides in the transgenic brain and retina

Aβ40 or Aβ42 peptide abundance in brain and retina was determined using ELISA as previously described [13,21,22]. Although Aβ40 and Aβ42 peptides were easily detected in Tg-AD or Alzheimer retina, in all instances, brain Aβ40 or Aβ42 peptide abundance far exceeded the level, which was found in any retina studied. Compared with age-matched controls, in human brain, the combined Aβ40 and Aβ42 peptide load was 26.3-fold higher in Alzheimer's disease, and the mean Aβ40 and Aβ42 peptide abundance was 9.7- fold higher in the AD brain compared with the AD retina. Each Tg-AD model has a variable age of senile plaque onset, with Tg2576 being the longest (10 months) and 5xFAD being the shortest (2 months; Table 1). The combined Aβ40 and Aβ42 peptide load in Tg-AD brain compared with retina was 16.5-fold, 116.1-fold, 64.3-fold, and 15.3-fold higher in Tg2576, PSAPP, 3xTg-AD, and 5xFAD models, respectively, indicating that Tg2576 and 5xFAD Tg-AD models have the highest retina-to-brain ratios of Aβ40 and Aβ42 peptides (Tables 1 and 2). Interestingly, the Tg-AD model that most closely approximated the human Aβ40 or Aβ42 peptide load in the retina was the 5xFAD model; the greatest ELISA-detectable abundances of Aβ40 and Aβ42 peptides in both the brain and retina were also detected in 5xFAD mice (Tables 1 and 2). Using both Aβpeptide deposition and CFH abundance as an index, these studies indicate that in Tg-AD models the degree of amyloidogenesis and inflammatory retinal pathology is in the order of 5xFAD> >Tg2576> >3xTg-AD> > >PSAPP, which roughly mimics the order of central nervous system (CNS)-specific expression of amyloid and synaptic pathology as reported in the source references and recent comparative studies (Table 1) [2,12,14–20].

Aβ42 peptides and complement factor H abundance

βAPP, Aβ42 peptide, and CFH levels were next measured in the retina of four Tg-AD models and along the whole retina/superior colliculus (SC)/PVC pathway in Alzheimer's disease brain (Figs 1 and 2). In the two Tg-AD models with the highest Aβ42 peptide abundance (Tg2576 and 5xFAD), we note an inverse relationship between the abundance of ELISA-detectable Aβ42 peptides and CFH (Fig. 1). This inverse relationship was also apparent along the retina/SC/PVC pathway (Fig. 2). These latter results indicate that high levels of neurotoxic Aβ42 peptides across the human visual pathway correlate with significant deficiencies in CFH, a major repressor of complement signaling, and hence increase the potential for proinflammatory signaling along this primary sensory route [4,8].

Discussion

During the course of mouse and human CNS development, ganglion cells of the retina and cortical neurons of the brain (forming at rates of up to 50 000 cells/s) derive from the prosencephalon and mesencephalon, respectively. The retina initially develops as an outpocketing of the neural tube, which invaginates to form the optic cup, the inner wall of which becomes the neural retina [7,9]. At maturity, a three-neuron chain, the retinal

NIH-PA Author Manuscript

NIH-PA Author Manuscript

NIH-PA Author Manuscript

photoreceptor, bipolar cell, and retinal ganglion cell, provides the initial visual pathway running from the sensory retinal photoreceptors through to the optic nerve; as few as two additional neurons carry visual signals through the SC to the PVC (Brodmann A17). Hence, retinal and brain cells of the anteroposterior axis of Tg-AD mice and Alzheimer's disease-affected visual circuitry were the anatomical pathways examined in this study.

Approximately 52 Tg-AD βAPP-overexpressing murine models, in which various βAPP generation and processing functions have been selectively altered, have been described (http://www.alzforum.org/res/com /tra/app/) [14–20]. In these Tg- AD models, the overexpressed human cell surface receptor and transmembrane glycoprotein βAPP (chr21q21.3) is readily cleaved by secretases to generate a number of neurotrophic or neurotoxic β-amyloid (Aβ) fragments. Beta-APP undergoes cleavage by α-secretase to yield a soluble APPαthrough the neurotrophic pathway, or by tandem β-secretase and γ-secretase cleavage to yield the neurotoxic Aβ40 and amyloidogenic Aβ42 peptides through the neurotoxic processing pathways [1–5,9]. Although most studies have involved examination of pathological changes in the murine Tg-AD limbic system, hippocampus, and brain cortex [14–20], fewer studies have examined proinflammatory mechanisms in the neural retina or in the visual signaling and processing system within the brain [9,13]. ELISA-based studies have previously found Aβ40 or Aβ42 peptides, as well as other unusual βAPP-derived peptide fragments, to be upregulated in the photoreceptors, retinal pigmented epithelium, inner nuclear layer, and ganglion cell layer of symptomatic Tg2576 mouse retina [13,14]. Interestingly, in age-related macular degeneration (AMD) and in stressed retinal pigmented epithelium cells, the lipofuscin fluorophore bis-retinoid A2E seems to be induced and is a major component of the AMD-associated drusen that also contains βAPP, Aβ40, Aβ42, and other βAPP-derived peptide fragments [7,9,24]. The γ-secretase PS2, essential for βAPP cleavage into toxic Aβ40 and Aβ42 peptides, is also induced in a stress-triggered model of retinopathy of prematurity and pathoangiogenesis [14]. The amyloidogenic, proapoptotic, and proinflammatory markers, βAPP, cyclooxygenase-2, cytosolic phospholipase A_2, and the apoptotic death protein DAXX, were similarly found to be significantly upregulated in the PVC of an advanced Alzheimer's disease brain, both at the level of RNA and protein, and these levels were observed to become progressively increased as the neuropathology of Alzheimer's disease progressively advanced [8,12].

Significant increases of Aβ42 peptides and decreases in CFH abundance in relation to age-matched controls in the aging retina of advanced Tg-AD models (Tg2576 and 5xFAD), and in the aging human visual circuitry indicate a surprisingly maintained inflammatory pathology across the anteroposterior retinal–cortical axis (Figs 1 and 2). Interestingly, CFH (chr 1q32), an internally repetitive glycoprotein and an important repressor protein known to contribute to the regulation of the brain's immune and inflammatory response, is found to be consistently downregulated, not only in Alzheimer neocortex [3,4,12] but also across the visual pathway in late-stage Alzheimer's disease (Fig. 2). CFH functions as a cofactor in the inactivation of its C3b ligand by factor 1 in the alternative complement pathway, and hence low ambient CFH levels are conducive to complement activation and inflammatory signaling in both the retina and brain [3–6,9]. CFH is also a molecular constituent of the drusen that accumulates in AMD and colocalizes with its ligand C3b in substructural spherules within drusen that also contains Aβ42 peptide, βAPP-derived fragments, CFH, and other complement proteins [4,15,24,25]. Moreover, the significant statistical relationship between the CFH Y402H 'risk' variant and the incidence of AMD may further suggest that either a defective 'mutant' CFH or low-CFH abundance may have analogous proinflammatory and AMD-promoting effects [3,24,25].

In summary, the 5xFAD Tg-AD model, as an imperfect transgenic model of Alzheimer's disease, exhibits the highest central nervous system-specific expression of amyloid and the

NIH-PA Author Manuscript

NIH-PA Author Manuscript

NIH-PA Author Manuscript

greatest extent of synaptic pathology [2,12,20]. The 5xFAD model also showed the highest concentration of Aβ40 and Aβ42 peptides and the lowest levels of CFH in the brain and retina (Figs 1 and 2). The fact that five pathogenic human genes drive Alzheimer-like pathology in the 5xFAD system [2,20] may help to explain the greater brain and retinal pathology in this particular Tg-AD model (Tables 1 and 2). Examination of other Tg-AD models, the effects of dietary manipulations such as high fat-cholesterol diets, and the contribution of each retinal cell layer to Aβ40 and Aβ42 peptide load and CFH abundance should further expand our understanding of brain and retinal patterns of inflammation and the pathogenic mechanism of their regulation throughout the visual circuitry.

Conclusion

Depending on the Tg-AD model, Aβ40 and Aβ42 peptides or the inflammatory marker CFH displayed variable expression in the aging transgenic retina. The observation was made that Aβ40 and Aβ42 peptide abundance and signals for the inflammatory–repressor, CFH, show an inverse correlation in advanced Tg-AD models of Alzheimer's disease, such as the 5xFAD model. Although murine eyes lack a distinct macular area, aging 5xFAD mice, may be suitable in-vivo models for studying the mechanisms of amyloidogenic and inflammatory neurodegeneration in the retina and how pathogenetic signals can progressively spread across the anteroposterior axis of the visual circuitry.

Acknowledgments

The authors thank Drs Chu Chen, Elizabeth Head, Wayne Poon, George Tejada, and Tommy Saing for Tg-AD mouse and human brain tissues or extracts and Darlene Guillot for expert technical assistance. Some of the brain tissues used in this study were provided by the Institute for Memory Impairments and Neurological Disorders and the University of California at Irvine Alzheimer's Disease Research Center; funding for the University of California at Irvine Alzheimer's Disease Research Center was provided by NIH/NIA Grant P50 AG16573. The author's work was further supported in part through Translational Research Initiative Grants from LSU Health Sciences Center New Orleans (W.J.L.) and an Alzheimer Association Investigator-Initiated Research Grant IIRG-09–131729 (W.J.L.).

References

1. O'Brien RJ, Wong PC. Amyloid precursor protein processing and Alzheimer's disease. Annu Rev Neurosci. 2010 [Epub ahead of print].
2. Philipson O, Lord A, Gumucio A, O'Callaghan P, Lannfelt L, Nilsson LN. Animal models of amyloid-beta-related pathologies in Alzheimer's disease. FEBS J. 2010; 277:1389–1409. [PubMed: 20136653]
3. Lukiw WJ, Zhao Y, Cui JG. An NF-κB-sensitive micro RNA-146a-mediated inflammatory circuit in Alzheimer disease and in stressed human brain cells. J Biol Chem. 2008; 283:31315–31322. [PubMed: 18801740]
4. Veerhuis R. Histological and direct evidence for the role of complement in the neuroinflammation of Alzheimer's disease. Curr Alzheimer Res. 2011; 8:34–58. [PubMed: 21143154]
5. Cui JG, Li YY, Zhao Y, Bhattacharjee S, Lukiw WJ. Differential regulation of interleukin-1 receptor-associated kinase-1 (IRAK-1) and IRAK-2 by miRNA- 146a and NF-kB in stressed human astroglial cells and in Alzheimer's disease. J Biol Chem. 2010; 285:38951–38960. [PubMed: 20937840]
6. Pogue AI, Li YY, Cui JG, Zhao Y, Kruck TP, Percy ME, et al. Characterization of an NF-κB-regulated, miRNA-146a-mediated down-regulation of complement factor H (CFH) in metal-sulfate-stressed human brain cells. J Inorg Biochem. 2009; 103:1591–1595. [PubMed: 19540598]
7. Lukiw WJ, Mukherjee PK, Cui JG, Bazan NG. A2E selectively induces COX-2 in ARPE-19 and human neural cells. Curr Eye Res. 2006; 31:259–263. [PubMed: 16531283]
8. Cui JG, Hill JM, Zhao Y, Lukiw WJ. Expression of inflammatory genes in the primary visual cortex of late-stage Alzheimer's disease. Neuroreport. 2007; 18:115–119. [PubMed: 17301674]

NIH-PA Author Manuscript

NIH-PA Author Manuscript

NIH-PA Author Manuscript

9. Wallace VA. Concise review: making a retina-from the building blocks to clinical applications. Stem Cells. 2011; 29:412–417. [PubMed: 21425405]
10. Kesler A, Vakhapova V, Korczyn AD, Naftaliev E, Neudorfer M. Retinal thickness in mild cognitive impairment and Alzheimer's disease. Clin Neurol Neurosurg. 2011 [Epub ahead of print].
11. Tippett WJ, Krajewski A, Sergio LE. Visuomotor integration is compromised in Alzheimer's disease patients reaching for remembered targets. Eur Neurol. 2007; 58:1–114. [PubMed: 17483579]
12. Li YY, Cui JG, Hill JM, Bhattacharjee S, Zhao Y, Lukiw WJ. Increased expression of miRNA-146a in Alzheimer's disease transgenic mouse models. Neurosci Lett. 2011; 487:94–98. [PubMed: 20934487]
13. Dutescu RM, Li QX, Crowston J, Masters CL, Baird PN, Culvenor JG. Amyloid precursor protein processing and retinal pathology in mouse models of Alzheimer's disease. Graefes Arch Clin Exp Ophthalmol. 2009; 247:1213–1221. [PubMed: 19271231]
14. Lukiw WJ, Gordon WC, Rogaev EI, Thompson H, Bazan NG. Presenilin-2 expression up-regulation in a model of retinopathy of prematurity and pathoangiogenesis. Neuroreport. 2001; 12:53–57. [PubMed: 11201091]
15. Hsiao K, Chapman P, Nilsen S, Eckman C, Harigaya Y, Younkin S, et al. Correlative memory deficits, Aβ elevation and amyloid plaques in transgenic mice. Science. 1996; 274:99–102. [PubMed: 8810256]
16. Holcomb L, Gordon MN, McGowan E, Yu X, Benkovic S, Jantzen P, et al. Accelerated Alzheimer-type phenotype in transgenic mice carrying both mutant amyloid precursor protein and presenilin 1 transgenes. Nat Med. 1998; 4:97–100. [PubMed: 9427614]
17. Kumar-Singh S, Pirici D, McGowan E, Serneels S, Ceuterick C, Hardy J, et al. Dense-core plaques in Tg2576 and PSAPP mouse models of Alzheimer's disease are centered on vessel walls. Am J Pathol. 2005; 167:527–543. [PubMed: 16049337]
18. Takeuchi A, Irizarry MC, Duff K, Saido TC, Hsiao Ashe K, Hasegawa M, et al. Age-related amyloid beta deposition in transgenic mice over-expressing both Alzheimer mutant presenilin 1 and amyloid beta precursor protein Swedish mutant is not associated with global neuronal loss. Am J Pathol. 2000; 157:331–339. [PubMed: 10880403]
19. Oddo S, Caccamo A, Shepherd JD, Murphy MP, Golde TE, Kayed R, et al. Triple-transgenic model of Alzheimer's disease with plaques and tangles: intracellular Aβ and synaptic dysfunction. Neuron. 2003; 39:409–421. [PubMed: 12895417]
20. Oakley H, Cole SL, Logan S, Maus E, Shao P, Craft J, et al. Intraneuronal beta-amyloid aggregates, neurodegeneration, and neuron loss in transgenic mice with five familial Alzheimer's disease mutations: potential factors in amyloid plaque formation. J Neurosci. 2006; 26:10129–10140. [PubMed: 17021169]
21. Lukiw WJ, Cui JG, Marcheselli VL, Bodker M, Botkjaer A, Gotlinger K, et al. A role for docosahexaenoic acid-derived neuroprotectin D1 in neural cell survival and Alzheimer disease. J Clin Invest. 2005; 115:2774–2783. [PubMed: 16151530]
22. Culicchia F, Cui JG, Li YY, Lukiw WJ. Upregulation of beta-amyloid precursor protein expression in glioblastoma multiforme. Neuroreport. 2006; 19:981–985. [PubMed: 18521005]
23. Cui JG, Zhao Y, Sethi P, Li YY, Mahta A, Culicchia F, et al. Micro-RNA-128 (miRNA-128) down-regulation in glioblastoma targets ARP5 (ANGPTL6), Bmi-1 and E2F-3a, key regulators of brain cell proliferation. J Neurooncol. 2010; 98:297–304. [PubMed: 19941032]
24. Fletcher EL, Jobling AI, Vessey KA, Luu C, Guymer RH, Baird PN. Animal models of retinal disease. Prog Mol Biol Transl Sci. 2011; 100:211–286. [PubMed: 21377628]
25. Thakkinstian A, Han P, McEvoy M, Smith W, Hoh J, Magnusson K, et al. Systematic review and meta-analysis of the association between complement factor H Y402H polymorphisms and age-related macular degeneration. Hum Mol Genet. 2006; 15:2784–2790. [PubMed: 16905558]

NIH-PA Author Manuscript

NIH-PA Author Manuscript

NIH-PA Author Manuscript

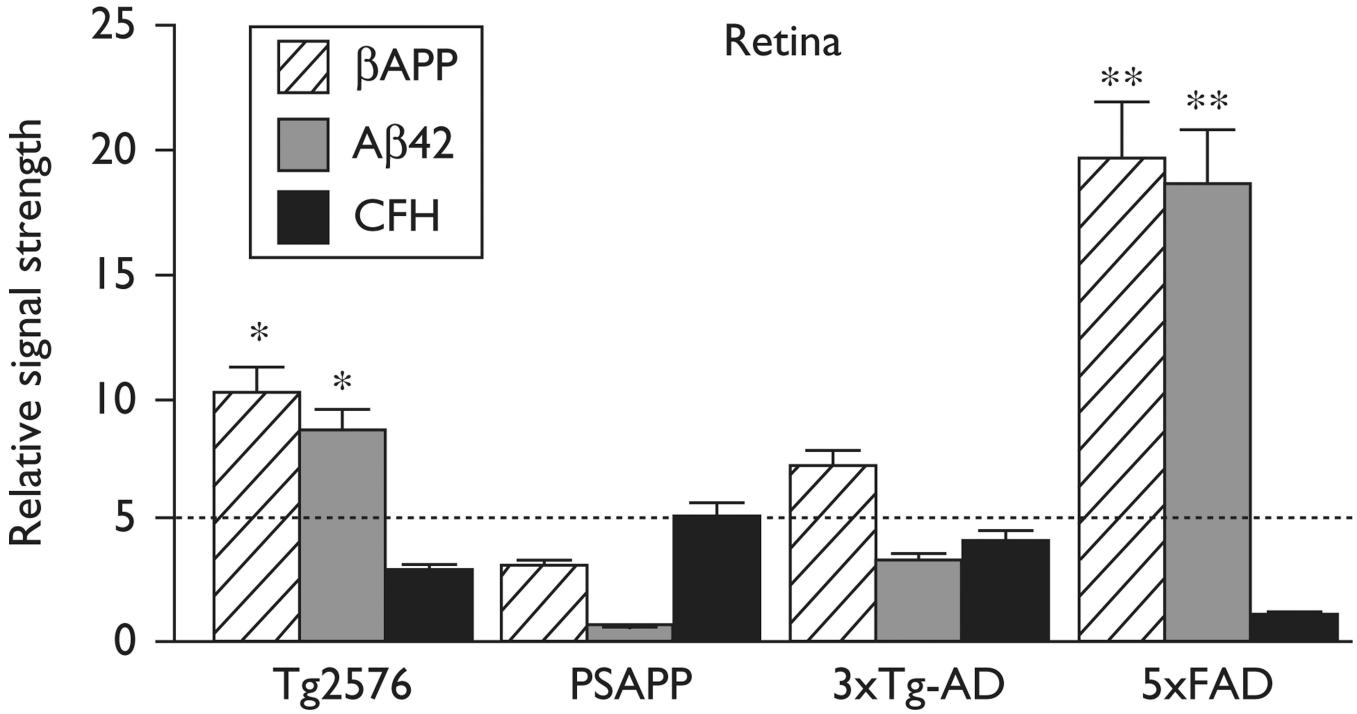

Fig. 1.

βAPP, Aβ42, and complement factor H (CFH) levels in transgenic murine models of Alzheimer's disease (Tg-AD) mouse retina compared with the age-matched controls. The presence of βAPP and Aβ42 peptides suggests a common and functional secretase-mediated processing of βAPP in the Tg-AD retina [8,12,13]; other βAPP-derived peptide fragments in Tg-AD retina have been described [13]. As further discussed in the text, highest relative βAPP, Aβ42, and the lowest relative CFH levels were found in 5xFAD retina. A dashed horizontal line at 5.0 indicates relative CFH levels in PSAPP mice for ease of comparison; N=5; *P<0.05; **P<0.01 (analysis of variance).

NIH-PA Author Manuscript

NIH-PA Author Manuscript

NIH-PA Author Manuscript

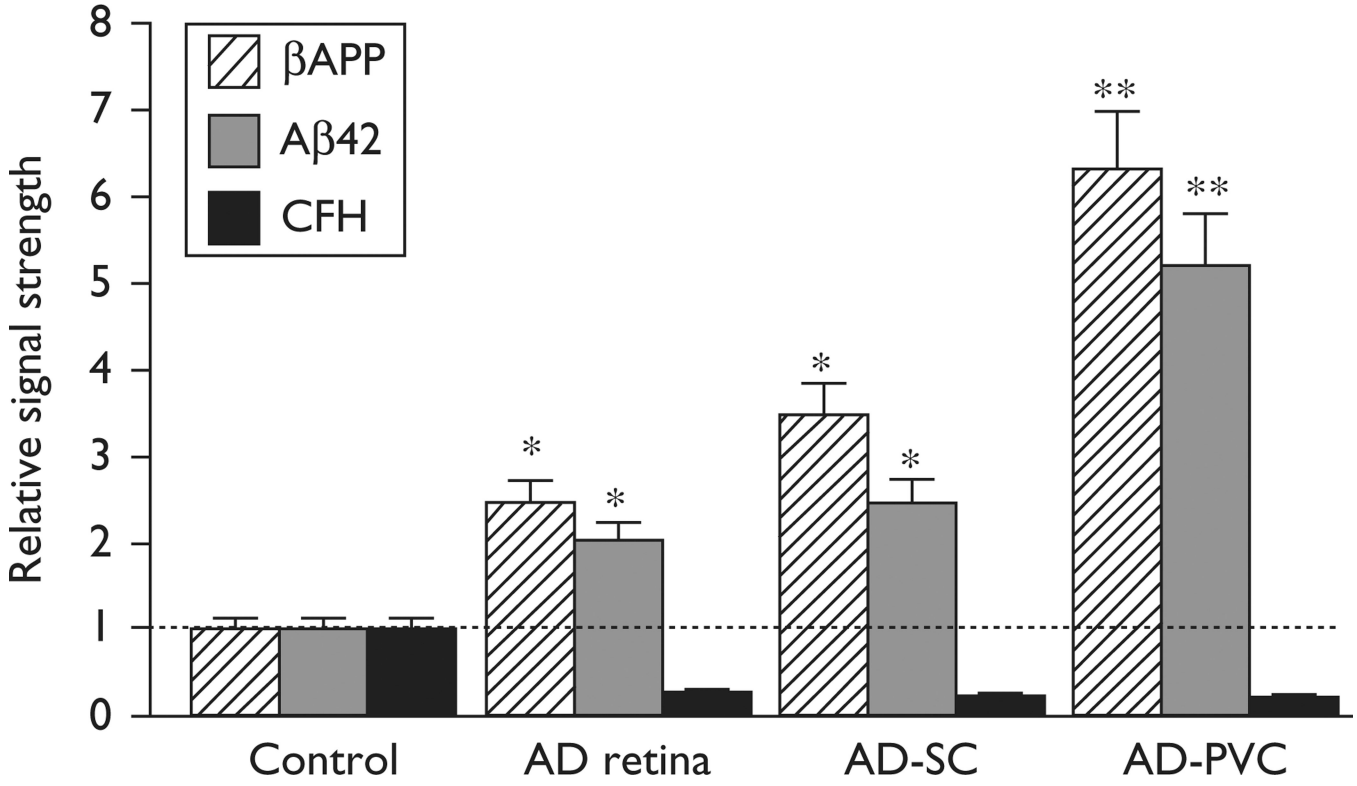

Fig. 2.

βAPP, Aβ42, and complement factor H (CFH) levels in the Alzheimer visual pathway. Data are shown for control, Alzheimer's disease retina (AD retina), Alzheimer's disease superior colliculus (AD-SC), and Alzheimer's disease primary visual cortex (AD-PVC; Brodmann area A17). The highest βAPP and Aβ42 peptide levels, averaging 19.1-fold to 15.5-fold over age-matched controls respectively, were found in the AD-PVC. A dashed horizontal line at 1.0 indicates relative βAPP, Aβ42 peptides, and CFH levels in age-matched control retina for ease of comparison; N=5; *P<0.05; **P<0.01 (analysis of variance).

NIH-PA Author Manuscript NIH-PA Author Manuscript NIH-PA Author Manuscript

Table 1

Transgenic murine models of Alzheimer's disease phenotype and neuropathological aspects of four transgenic murine models of Alzheimer's disease derived from the original 'source' references and unpublished data [12,14–20]

Tg-AD model	Strain[a]	Age of SP onset[c]	Tg-AD promoter/transgene[d]	SPD[e]	CNS[f]	Synaptic pathology[g]	Retinal pathology[h]	Source reference
Tg2576	C57B6J X SJL F1 hybrid[b]	10	Hamster prion promoter/human APP695 cDNA with K670N/M671L	+ + + +	+ +	+ + +	+ +	[2,8,12,15]
PSAPP	C57BL6/D2AF[a]	6	Tg2576×PSEN1M146L	+ +	+	–	+	[2,16–18]
3xTg-AD	Hybrid 129/ C57BL6[a]	6	Thy1 promoter/APP695-Swedish/Tau isoform 4R0N(P301L mutation)/ PSEN1M146L	+ +	++ + +	+	+	[2,12,19]
5xFAD	C57BL6/SJL[b]	2	Thy1 promoter/B6SJL-Tg(APPSwFlLon,PSEN1M146L*L286V)6799Vas/J	+ + + +	+ + + +	+ + + +	+ + + +	[2,12,20]

These studies are the first to comparatively analyze Aβ peptide levels in the retina in four different transgenic murine models of Alzheimer's disease (Tg-AD) models; Aβ peptide levels in the brain are comparable with several previous studies [15–22]. Symptomatic Tg-AD models exhibit variable senile plaque density [SPD; as seen anywhere within the central nervous system (CNS) in aged Tg-AD mice], and synaptic neuropathology (as determined by microscopic and molecular abundance measures; see below; unpublished observations); +detected, + + moderate abundance, + + + high abundance; + + + + extensive phenotype; see also references [2,12,14–20]. The scoring system adapted from [2,12], also took into consideration additional Tg-AD characteristics listed at the Tg-AD website http://www.alzforum.org/res/com/tra/app/default.asp, in addition to observed deficits in the abundance of several key cytoarchitectural and synaptic support proteins, including neurofilament light chain, spectrin, synaptophysin, synapsin-2, and syntenin (data not shown) [2,12], and from observations made in the original source reference for each Tg-AD type (rightmost column).

Table revised and modified from references [2,8,12,15–20].

[a]Genetic background strain.

[b]Tg2576 and 5xFAD mice are generated from C57B6JxSJLF1 and C57Bl6/SJL hybrids, but only age-matched C57BL6/SJL and C57BL6 control mice were analyzed for Aβ40 and Aβ42 peptide abundance in these studies (see Table 2; http://www.alzforum.org/res/com/tra/app/TGCRND8.asp http://www.alzforum.org/res/com/tra/app/).

[c]Onset (in months) of first appearance of senile plaques (SP) [2,8,12,15–20].

[d]Individual Tg-AD promoter constructs are described in more detail in source references (right-most column).

[e]SPD (highest SPD per mm^2 observed) and determined as previously described [21].

[f]CNS-specific expression of amyloid [2,15–20].

[g]Synaptic pathology (loss of synaptic structure) scored as in source references and references [12,18,20].

[h]Retinal pathology is scored by cumulative Aβ40 peptide or Aβ42 peptide load as described in Table 2 (right-most column).

NIH-PA Author Manuscript

NIH-PA Author Manuscript

NIH-PA Author Manuscript

Table 2

Aβ40, Aβ42, and Aβ40 and Aβ42 peptide levels in human and transgenic murine models of Alzheimer's disease brain and retina

Tissue	*N*	Aβ40 peptide (pmol/g protein)	Aβ42 peptide (pmol/g protein)	Aβ40 and Aβ42 (pmol/g protein)
Human control neocortex	6	22.4 ±9.4	56.3 ±11.5	78.7
Human AD neocortex	6	144.5 ±66.8 *	1529 ±222 **	2073.5 **
Human AD retina	3	11.5 ±1.1	201.4 ±112 *	212.9 *
C57BL6 control brain	3	1.25 ±0.7	1.51 ±0.8	2.76
C57BL6/SJL control brain	3	2.13 ±1.1	14.15 ±2.01	16.28
C57Bl6/SJL control retina	3	1.05 ±0.8	2.45 ±4.51	3.5
Tg2576 brain	5	263 ±563 *	1200 ±234 **	1463 *
PSAPP brain	5	767 ±321 **	1534 ±450 **	2301 **
3xTg-AD brain	5	817 ±224 **	1384 ±158 **	2201 **
5xFAD brain	5	861 ±451 **	1966 ±328 **	2827 **
Tg2576 retina	4	1.26 ±0.8	85 ±39 *	86.26 *
PSAPP retina	3	1.61 ±1.1 *	18.2 ±1.8 *	19.82 *
3xTg-AD retina	5	1.22 ±0.2	33.1 ±16.1 *	34.22 *
5xFAD retina	6	3.6 ±1.5 **	181 ±112 **	184.6 **

Age-matched control retinal tissues from transgenic murine models of Alzheimer's disease (Tg-AD) mice showed Aβ40 or Aβ42 of less than 1 pmol/g of tissue (below the detection limit of the enzyme-linked immunosorbent assay of 1 pmol/g of protein) [21]; statistical analysis of Aβ40 and Aβ42 peptide includes the mean pmol/g of protein for the *N* (number analyzed) for each tissue, and one standard deviation from that mean; the combined Aβ40 and Aβ42 peptide abundance (right-most column) is an arithmetic sum of individual Aβ40 and Aβ42 peptide mean abundances.

* $P<0.05$. Significance over-respective controls are indicated.

** $P<0.01$. Significance over-respective controls are indicated (analysis of variance) [2,12,21].